# Part II: Laser-Doppler Measurements of Turbulent Structure

**W. D. McCOMB and L. H. RABIE**

School of Engineering
University of Edinburgh
Edinburgh, Scotland

Aqueous solutions of polyethyleneoxide (Polyox WSR-301) were injected into a pipe flow through either a small tube at the center line or an annular slot in the wall. The solution contained polymer at an injection concentration of 1,000 wppm. Injection into water flow with a Reynolds number Re = $3.5 \times 10^4$ was at a rate which gave a mean polymer concentration of 5.0 wppm in the water flow. A laser-Doppler anemometer (LDA) was used to measure the streamwise turbulent velocity at various radial positions and at several stations downstream from the injection point.

Results were obtained for mean velocity and intensity profiles; autocorrelations; and one-dimensional energy spectra. The mean bursting period was determined using the "short-sampling-time" autocorrelation method. Changes in all these quantities due to polymer injection were found to depend on the amount of local drag reduction at that particular downstream station but were independent of the local polymer concentration at the measuring point.

## SCOPE

It is well known that certain long-chain polymers in solution can reduce turbulent frictional drag below that for the solvent alone. In a previous paper (Part I) we argued that the possibility of developing permanently drag-reducing surfaces rested on our possessing a detailed picture of the way the dissolved polymers modify the turbulence. Further, by injecting polymer solutions into pipe flow, and relating the development of local drag reduction to the way in which the polymer spread out as it was carried downstream, we were able to identify a narrow annulus near the wall as the region where the polymer interacted with the turbulence.

The aim of the present work was to use a laser-Doppler anemometer to measure the detailed turbulent structure of the flow; both before, and during, injection of the polymer solutions. By measuring quantities such as the mean velocity, turbulent intensity and autocorrelations, as functions of radial position and distance downstream from the injector, we could hope to achieve two main objectives. First, we could further test the conclusion from Part I that the additives are only effective within a narrow annulus in the cross-section of the flow. Second, we could find out whether drag reduction by injection of polymer solutions (inhomogeneous drag reduction) is the same basic phenomenon as drag reduction in premixed polymer solutions (homogeneous drag reduction).

## CONCLUSIONS AND SIGNIFICANCE

1. The presence of drag-reducing polymer additives outside the near-wall region had no discernible effect on the flow structure.

2. The presence of polymer additives in the near-wall region resulted in significant changes in the whole structure of the flow. These changes may be seen in the core, even when that region is free from polymer additives.

3. The change in flow structure is demonstrated by:

(a) The presence of the polymer interactive layer in the mean velocity profile

(b) An increase in the axial turbulent intensities near the wall. This increase extended to the center line as the drag reduction increased

(c) A substantial increase in the mean time between bursts

(d) A reduction of the energy in the small scales of the turbulence. Correspondingly, there was a decrease in the rate of dissipation and an increase in the size and lifetime of the turbulent eddies

Overall, these results support the conclusion from Part I that the polymers interact with the turbulence in an effective annulus which is *near* but not *at* the wall. They also establish the unimportance of polymer concentration in regions of the flow which are outside this effective annulus. Furthermore, comparisons with other LDA measurements taken in homogeneous solutions strongly support the view that drag reduction produced by polymer injection is not different from homogeneous drag reduction. Thus the drag reduction at any given time, in either type of flow, depends only on the concentration and condition of the polymer in the effective annulus at that time.

### INTRODUCTION

In part I of this investigation (McComb and Rabie, 1982), we described the streamwise evolution of the local drag reduction following the injection of concentrated polymer solutions at the centerline and the wall of the pipe. At the same time, the radial dispersion of the polymers under the action of turbulent diffusion was established by measuring concentration profiles at various streamwise distances from the injection point. Here, we describe the streamwise change in turbulent structure following the injection of polyethyleneoxide (Polyox WSR-301). In particular, we report LDA measurements of mean velocity profiles; streamwise turbulent intensity profiles; streamwise autocorrelations and one-dimensional energy spectra; and the mean time between bursts. First we discuss other LDA measurements in non-Newtonian and drag-reducing flows.

The first use of LDA in drag-reducing flows to obtain a comprehensive set of results was by Rudd (1971), who used a 12.7 × 12.7 mm$^2$ duct. He found that the axial turbulent intensities were increased, compared to values for water flows. Logan (1972) also used LDA to measure Reynolds stresses in a 12.7 × 12.7 mm$^2$ duct and found increased axial turbulent intensities near the wall in drag-reducing flows. However, in both these cases the presence of secondary flows due to the square cross-section must raise

Correspondence concerning this paper should be addressed to W. D. McComb. L. H. Rabie is now at Mechanical Engineering Department, Mansoura University, Egypt.

0001-1541-82-6095-0558-$2.00. 

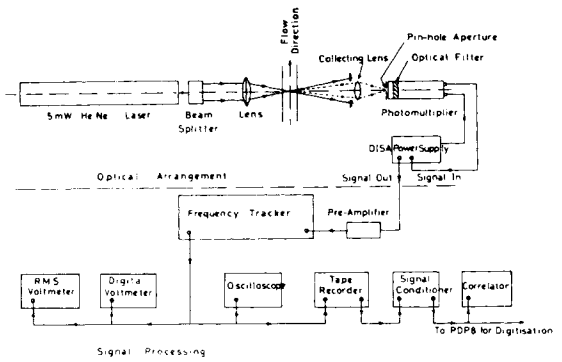


**Figure 1. Optical arrangement and signal processing chain.**

questions about the relevance of the results to pipe flows. Later measurements by Reischman and Tiederman (1975) in a channel flow, where the duct cross-section had a high aspect ratio, showed some differences of detail from those taken in square ducts. We shall return to this point when discussing our own results.

LDA measurements in round pipes have been reported by Chung and Graebel (1972) and by Mizushina and Usui (1977). In the first of these, axial intensities were found to be reduced by the polymer additives (although refraction errors limited the reliability of the results other than in the core region of the pipe). In the second case, axial intensities were reduced by polymer additives near the wall. But reduced values were also obtained near the wall in water flow and this was attributed to the rather large LDA probe (or scattering) volume.

Finally, McComb et al. (1977) used LDA to measure one-dimensional spectra in grid-generated turbulence of polymer solutions.

## EXPERIMENTAL APPARATUS AND PROCEDURE

### Flow System

The test section was a 6 m long × 26 mm i.d. horizontal Perspex pipe which formed part of an open-loop water flow system. Polymer solutions were injected at the beginning of the test section where, following an entrance length, well-developed turbulent flow was already established.

Full details of the flow system, injection system and preparation of polymer solutions have been given in Part I.

### Laser-Doppler Anemometer

The LDA was used in the real-fringe, forward scattering mode. This arrangement was chosen for its ease of alignment and the ability to combine high spatial resolution with good signal-to-noise ratio.

The optical arrangement is shown in Figure 1. The light from a 5 mW He-Ne laser (Spectra-Physics, model 120) was divided into two parallel beams of equal intensity, in the horizontal plane, by a prism beam-splitter (Precision Devices, Malvern). The distance between the two parallel beams was kept at 24.5 mm. The two beams were focused to form a fringe pattern at the measuring point using a lens with a focal length of 51 mm. The measuring or probe volume is defined by the intersection of the two beams. The angle between the beams was 28° which resulted in the parameters of the probe volume being as follows:

(a) The fringe spacing was 1.3 $\mu$m.

(b) The probe volume dimensions were 31, 130 and 32 $\mu$m in the streamwise, radial and spanwise directions, respectively.

(c) There were 25 fringes in the measuring volume.

(d) For this configuration, the Doppler frequency $f_D$ was 760 kHz for a velocity of one metre per second.

The scattered light from the probe volume was collected by a lens of 121 mm focal length which was mounted on the front of the photomultiplier (DISA 55L 12). The power supply of the photomultiplier (PM) was a DISA high voltage supply, type 55L15. The output of the PM was connected to a signal processing system which will be described in the next section.

The photomultiplier was aligned with the bisector of the two incident beams, as this is the direction of the maximum intensity of the scattered light. The collected light was focused on a small pinhole of 0.1 mm diameter in front of the PM tube. A narrow band-pass interference filter, which was centered on 633 mm (the wavelength of the He-Ne laser light), was attached to the PM tube housing. This reduced the noise level from ambient light.

Because of the low concentration of natural scattering particles in the flow, it was necessary to seed the flow with milk. A good signal-to-noise ratio was obtained at a milk concentration of 100 wppm. The average fat particle size is about 0.3 $\mu$m with $10^{14}$ particles per liter of milk (George and Lumley 1973). Thus the particle concentration in the flow was about $10^7$ particles per $cm^3$.

### Signal Processing

The signal processing chain is also shown in Figure 1. A frequency tracker (Communications and Electronics Ltd., model HF) was used to convert the Doppler frequency from the photomultiplier into a voltage proportional to the instantaneous velocity. A digital voltmeter (DISA, type 55D31) was used to obtain mean values of the output voltage from the tracker (and hence the mean flow velocity). Similarly, an RMS voltmeter (DISA, type 55D35) was used to obtain the intensity of the turbulent fluctuations in the streamwise direction. In both cases, the instrument time constant was set to 10 seconds.

The instantaneous voltage from the frequency tracker was also recorded on a Racal-Thermionic Store 4D tape recorder. The recording speed was 38 cm/s which ensured a flat frequency response up to 5 kHz. Recorded signals were played back at recording speed and the output was connected to a low-pass filter (DISA Signal Conditioner, type 55D26), with a cut-off frequency of 2.5 kHz.

The output from the low-pass filter was further processed in two ways. The autocorrelations (and hence the mean bursting time) were obtained using a correlator (Hewlett-Packard 3721A). The output of the signal conditioner was also digitized at 5,000 samples/s, using an A/D converter and PDP8 minicomputer. The digitized data were transferred to the ICL 4/75, where energy spectra were calculated using the Fast Fourier Transform (FFT).

The system for obtaining the spectrum is essentially the same as that described previously in McComb et al. (1977), where discussions of ambiguity noise and spectral resolution limits will also be found.

## RESULTS AND DISCUSSION

LDA measurements were first made in turbulent water flow without polymer injection. This was to check the performance of the system and establish that the injection process itself did not affect the measurements. Details will be found in the thesis by Rabie (1978). However, in the figures to be given for results with polymer injection, a curve for water alone is generally included for comparative purposes.

The polymer used was polyethyleneoxide (Polyox WSR-301) at an injection concentration of $C_p$ = 1,000 wppm. The injected solutions contained salt (NaCl) at a concentration of $C_s$ = 2,000 wppm, to ensure strict comparability with the results in Part I, where it was needed as a tracer for diffusion measurements. In all cases, the polymer solutions were injected into a water flow with a constant Reynolds number Re = $3.5 \times 10^4$ and for all tests the injection rate was such that the average polymer concentration in the flow was $C_{av}$ = 5.0 wppm.

When the injection was at the centerline, measurements were taken over a number of cross-sections at different distances downstream from the injection point. These distances ranged from

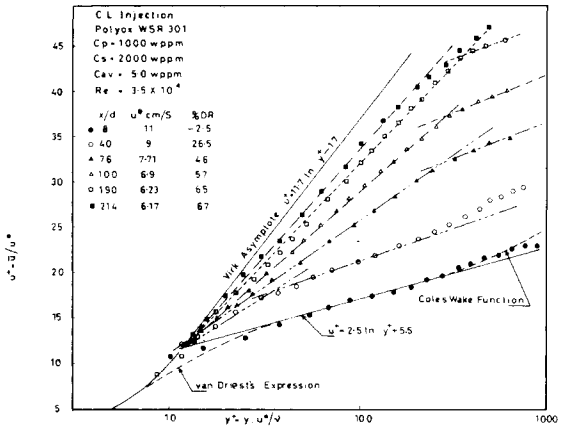


(a) Injection at the centerline

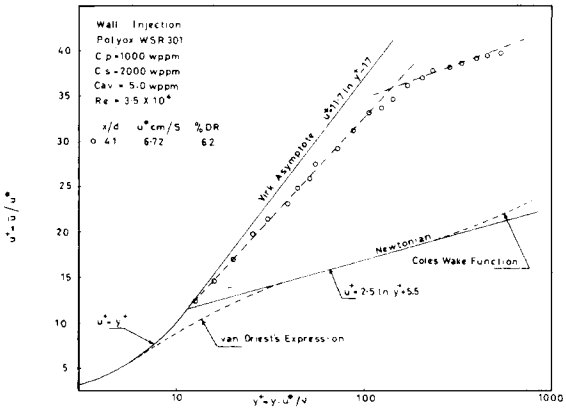


(b) Injection at the wall

**Figure 2. Mean velocity profiles during the injection of Polyox WSR-301.**

8 diameters (where the drag was slightly increased and the polymer was still in the core region of the flow) to 214 diameters from the injector (where the asymptotic drag reduction was obtained and the polymer molecules were uniformly distributed over the cross-section of the pipe).

Only one set of measurements was made for injection at the wall. These were made over a cross-section at 41 diameters downstream from the injector. At this section, the local drag reduction was 62.5% and there was no polymer in the core region of the flow.

### Mean and RMS Velocity Profiles during Polymer Injection

Before taking the LDA measurements at any station the local drag reduction was measured in order to calculate the local value of the friction velocity $u^*$ at that position. The results for velocities were then normalized using the local friction velocity and the kinematic viscosity $\nu$ of water at the flow temperature.

The latter step is very much a practical expedient. For, where the polymer concentration is nonuniform across a section, one may expect a corresponding variation in solution viscosity. However, the worst case is the point nearest the injector, where local polymer concentration varied from 110 wppm at the centerline to zero near the wall. Measurements of solution viscosity at different polymer concentrations (e.g., McComb et al., (1977) where a similar problem was encountered in connection with the scaling of spectra) indicate that this variation from the value of $\nu$ for water was less than 10%. At the next downstream station the variation in solution viscosity was less than 4% of $\nu$ for water. By the time the largest downstream distances were reached, the solution viscosity was virtually constant and indistinguishable from that of water.

Mean velocity profiles for centerline injection and for injection at the wall are plotted in Figures 2(a) and 2(b), respectively. RMS velocity profiles are presented in Figs. 3(a) and 3(b) for centerline injection and in Figures 3(c) and 3(d) for injection at the wall.

TABLE 1. CONSTANTS OF MEAN VELOCITY PROFILES

| Test | $x/d$ | $u^*$(cm/s) | %$DR$ | $A^1$ | $B^1$ | $C^2$ | $D^2$ |
|---|---|---|---|---|---|---|---|
| C.L. Inj. | 8.0 | 11.0 | −2.5 | 2.5 | 5.5 | — | — |
| C.L. Inj. | 40.0 | 9.00 | 26.5 | 2.8 | 8.4 | 5.9 | −2.8 |
| C.L. Inj. | 76.0 | 7.70 | 46.0 | 3.6 | 12.0 | 6.3 | −3.3 |
| C.L. Inj. | 100.0 | 6.90 | 57.0 | 3.7 | 16.5 | 8.0 | −7.8 |
| C.L. Inj. | 190.0 | 6.23 | 65.0 | 3.4 | 24.5 | 9.7 | −12.3 |
| C.L. Inj. | 214.0 | 6.17 | 67.0 | — | — | 10.2 | −13.5 |
| Wall Inj. | 41.0 | 6.72 | 62.0 | 3.2 | 20.0 | 9.8 | −12.6 |

[1] Mean velocity profile in the core region:

$$U^+ = A \ln y^+ + B$$

[2] Mean velocity profile in the polymer interaction region:

$$U^+ = C \ln y^+ + D$$

The results for mean velocity are in broad agreement with velocity profiles measured in homogeneous drag reduction. In particular, they agree well with the results of Reischman and Tiederman (1975) in the following respects:

(a) Figures 2(a, b) confirm the existence of three regions in drag-reducing turbulent flow. These are the viscous sublayer, the polymer-interaction layer, and the turbulent core region.

(b) The (nondimensional) thickness of the viscous sublayer was the same as that in Newtonian flow.

(c) The slope of the mean velocity curve in the polymer interaction layer depended on the amount of drag reduction.

The mean velocity profiles may be compared to the well known universal law

$$U^+ = A \ln y^+ + B, \tag{1}$$

where $A = 2.5$ and $B = 5.5$ for Newtonian fluids, and the ultimate profile of Virk et al. (1970)

$$U^+ = 11.7 \ln y^+ - 17, \tag{2}$$

which is associated with the maximum drag-reduction asymptote. The polymer-interaction layer was found to extend from $y^+ = 12$, which is the point of intersection of the ultimate profile with the universal law, to the core region. The mean velocity in this region can be described by:

$$U^+ = C \ln y^+ + D. \tag{3}$$

The values of the constants $C$ and $D$ were calculated for each profile and are presented in Table 1, along with corresponding values of $A$ and $B$ for the core region.

Two further points about the results merit a specific mention. First, in Figure 2(a), the profile at $x/d = 8$ is taken in a region of slight drag increase and is virtually identical to that for water. At this station there was a substantial concentration of polymer in the core region but it had not yet reached the wall. In general terms, it is clear from the other profiles (taken in conjunction with the results of Part I) that changes in the mean velocity profile developed with the amount of drag reduction (i.e., the amount of polymer in the wall region).

In addition, this particular result indicates that the injection process itself has no effect on the velocity profile.

Second, in Figure 2(b) we have the reverse situation. The polymer at this point was still confined to the wall region (Part I) while the drag reduction was rather large at about 62%. The velocity profile was found to be consistent with those measured during centre-line injection and even showed some modification in the turbulent core (Table 1). Thus the influence of the drag reduction extends to the flow in the core even although the core was almost free of polymer. On the other hand, the presence of large concentrations of polymer in the core has little or no effect on the mean velocity. It therefore seems that the local presence of polymer molecules outside the effective annulus is not a controlling factor.

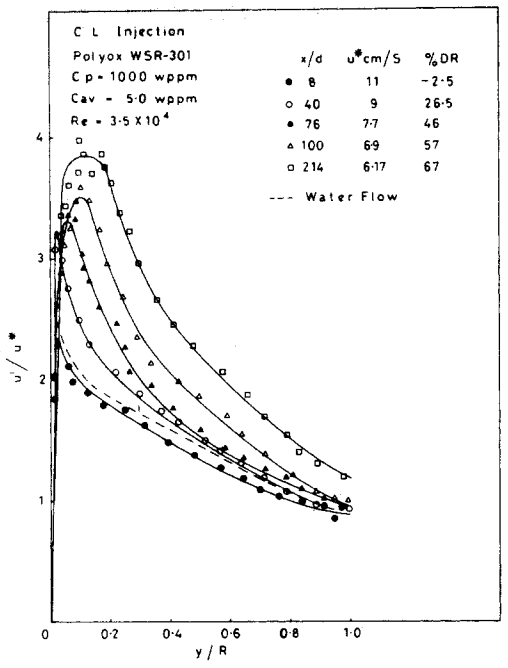


(a) Injection at centerline as a function of $Y/R$

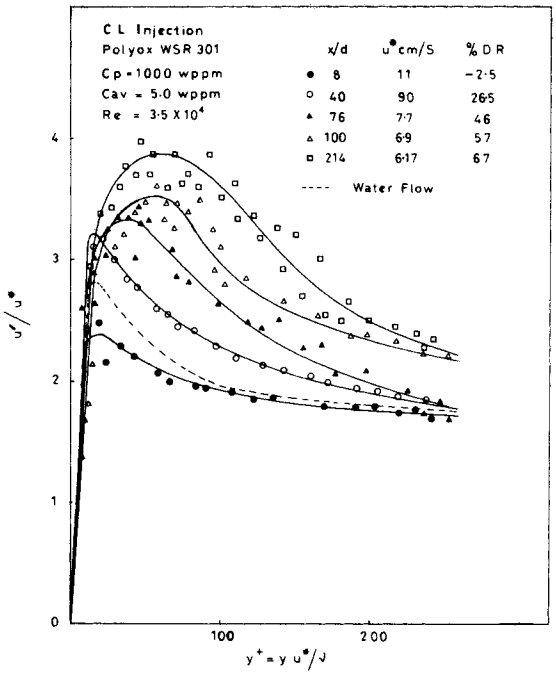


(b) Injection at centerline as a function of $y^+ = yu^*/\nu$

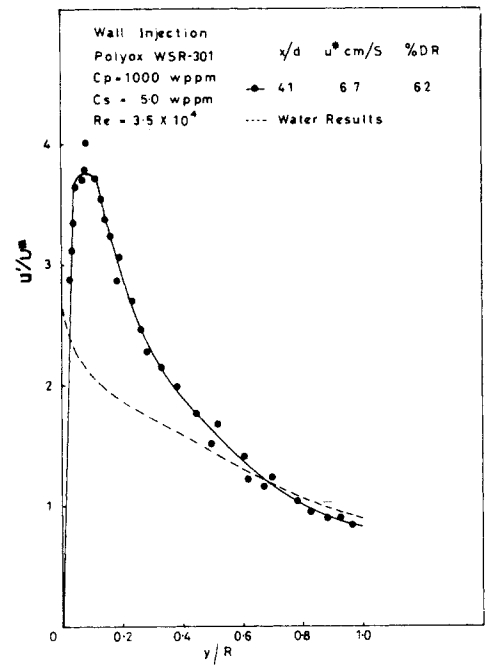


(c) Injection at wall as a function of $y/R$

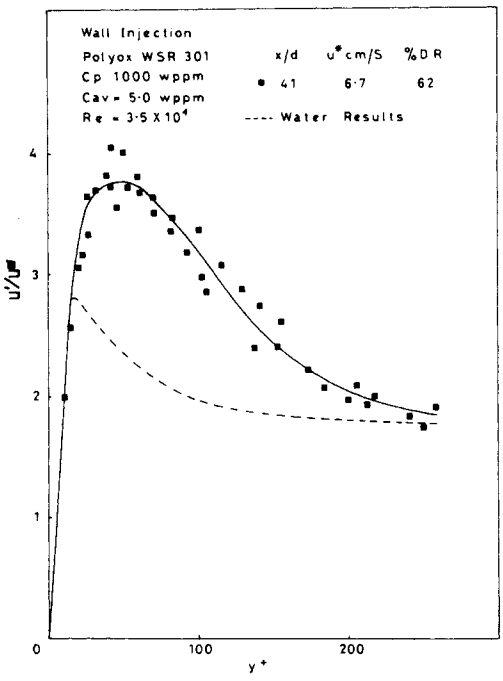


(d) Injection at wall as a function of $y^+ = yu^*/\nu$

**Figure 3. Turbulent intensity profiles during injection of Polyox WSR-301.**

The results for the RMS velocity profiles were generally consistent with the above discussion for the mean velocity. In Figure 3(a), it can be seen during injection at the centerline, the value of $u'/u^*$ increased in the wall region. As the percentage of drag reduction increased, the corresponding increase in $u'/u^*$ extended out from the wall. At the largest drag reduction, there was an appreciable increase in the RMS velocity at the centerline. When plotted against $y^+$ to show behaviour in the wall region in Figure 3(b), the peak of intensity (which is quite sharp in Newtonian flows) was found to spread out. This effect was previously noted by Reischman and Tiederman (1975).

The results for injection at the wall, as shown in Figure 3(c, d), were quite consistent with those for injection at the centerline. However, an interesting difference was the slightly lower value of $u'/u^*$ in the turbulent core. This rather small effect was the only evidence for a local dependence on polymer concentration near the centerline of the pipe.

### Effect of Polymer Injection on Streamwise Autocorrelations

Autocorrelation of the streamwise velocity fluctuations was carried out using the Hewlett-Packard correlator (Model 3271A). Values of the autocorrelation coefficient $R_{11}(\tau)$ taken at various downstream stations (with corresponding variations in local drag reduction) are shown as a function of time delay in Figures 4(a) and 4(b) for $r/R = 0.0$ and 0.88, respectively.

The most obvious feature of the results is the increase in the macroscale (integral time scale) where there is substantial local drag

TABLE 2. RATE OF TURBULENT DISSIPATION AND DISSIPATION LENGTH AND TIME SCALES

| Test | $x/d$ | $\%DR$ | $u^*$ cm²/s | $\nu$ cm²/s | $r/R = 0.0$ $\epsilon$ cm²/s³ | $\eta_d \times 10^3$ cm | $\tau_d \times 10^3$ s | $r/R = 0.85$ $\epsilon$ cm²/s³ | $\eta_d \times 10^3$ cm | $\tau_d \times 10^3$ s |
|---|---|---|---|---|---|---|---|---|---|---|
| Water Flow | — | — | 10.5 | 0.014 | 1510 | 6.7 | 3.1 | 14260 | 3.8 | 1.0 |
| C.L. Inj. | 8 | −2.5 | 11.0 | 0.015 | 1500 | 6.9 | 3.1 | 15070 | 3.8 | 1.0 |
| C.L. Inj. | 40 | 26.5 | 9.0 | 0.015 | — | — | — | 9670 | 4.3 | 1.3 |
| C.L. Inj. | 76 | 46.0 | 7.7 | 0.015 | 253 | 10.7 | 7.7 | — | — | — |
| C.L. Inj. | 100 | 57.0 | 6.9 | 0.015 | 165 | 12.0 | 9.5 | 3840 | 5.4 | 2.0 |
| C.L. Inj. | 214 | 67.0 | 6.17 | 0.015 | 157 | 12.1 | 9.8 | 2960 | 5.8 | 2.3 |
| Wall Inj. | 41 | 62.0 | 6.7 | 0.015 | 160 | 12.1 | 9.7 | 3670 | 5.5 | 2.1 |

$\eta_d$ = dissipation length scale = $(\nu^3/\epsilon)^{1/4}$
$\tau_d$ = dissipation time scale = $(\nu/\epsilon)^{1/2}$

reduction. Increased macroscales have previously been reported in homogeneous drag reduction where measurements were based on electrochemical mass transfer techniques (e.g., Butson and Glass, 1974; Hanratty et al., 1977).

In Figure 4(a), autocorrelation curves measured at the centerline of the pipe are shown. The importance of this comparison lies in the experimental conditions under which these measurements were carried out. The results for $x/d = 8$ were taken where the polymer concentration was very high but there was no drag reduction. The result was not very different from that for water. On the other hand, at $x/d = 214$, the concentration at the centerline was about 5 wppm and the drag reduction was about 67%. Here the decay rate of the correlation curve was very much reduced. For $x/d = 41$ with injection at the wall, the centerline concentration was low (actually, too low to be measurable) and the drag reduction large (62%), very similar results were obtained.

Again, these results strongly suggest that the turbulence structure is unaffected by local polymer concentration. It is seemingly determined entirely by the degree of drag reduction which implies a dependence on concentration in the effective annulus only (Part I).

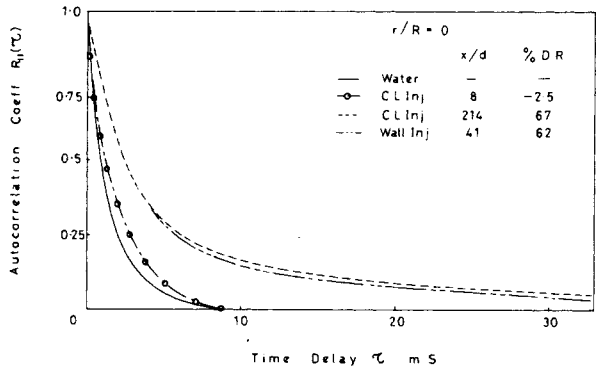


(a) $r/R = 0$

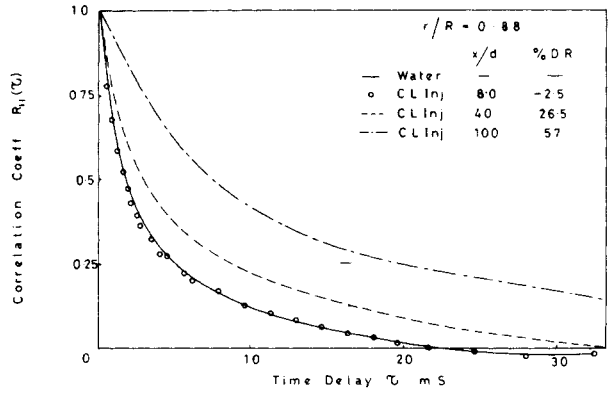


(b) $r/R = 0.88$

**Figure 4. Autocorrelation of the streamwise fluctuating velocity $R_{11}(\tau)$ at various radial positions.**

TABLE 3. BURSTING TIME RESULTS

| Test | $\%DR$ | $u^*$ cm/s | $\nu$ cm²/s | $\frac{T_B}{s}$ | $\frac{T_B \cdot u^{*2}}{\nu}$ | $\frac{T_B \cdot U}{R}$ |
|---|---|---|---|---|---|---|
| Water Flow | — | 11.0 | 0.013 | 0.028 | 255 | 5.5 |
| Water Flow | — | 9.7 | 0.011 | 0.029 | 248 | 5.3 |
| Water Flow | — | 10.5 | 0.014 | 0.035 | 266 | 6.8 |
| C.L. Inj. | −2.5% | 11.0 | 0.015 | 0.034 | 274 | 6.6 |
| C.L. Inj. | 26.5% | 9.0 | 0.015 | 0.094 | 500 | 18.0 |
| C.L. Inj. | 46% | 7.7 | 0.015 | 0.175 | 690 | 36.0 |
| C.L. Inj. | 57% | 6.9 | 0.015 | 0.250 | 795 | 52.5 |
| C.L. Inj. | 65.0% | 6.23 | 0.015 | 0.380 | 980 | 83.0 |
| C.L. Inj. | 67.0% | 6.17 | 0.015 | 0.455 | 1160 | 102.0 |
| Wall Inj. | 62.0% | 6.7 | 0.015 | 0.430 | 1280 | 89.0 |

Other results obtained also confirm this behaviour and show that it extends into the wall region.

### Effect of Polymer Injection on Streamwise Energy Spectrum

As discussed before, the analogue output of the frequency tracker was recorded on magnetic tape. The recorded signal was played back, low-pass filtered (cutoff frequency 2.5 kHz), digitized at a sample rate of 5 kHz, and fed to the computer to calculate the one-dimensional energy spectrum in the frequency domain using the FFT algorithm. This resulted in $E(f)$ where $E$ is the energy spectrum and $f$ is the frequency in Hz.

The spectrum was transformed to the wavenumber domain using:

$$k = \frac{2f}{U} \tag{4}$$

where $U$ is the mean velocity and $k$ is the wavenumber. Then two methods of scaling the results were adopted. First, spectra were normalized using the local RMS velocity $u'$ and the diameter of the pipe, $d$. Thus, normalized spectra $E(k)u'^2d$ were plotted against nondimensional wave-number $k_d$.

Second, spectra were scaled using the well known Kolmogoroff variables: this method allowed us to compare spectra at the same value of water shear stress. The Kolmogoroff dissipation wave-number $k_d$ is given by:

$$k_d = (\epsilon/\nu^3)^{1/4} \tag{5}$$

where $\nu$ is the kinematic viscosity and $\epsilon$ is the rate of dissipation of turbulent energy.

The kinematic viscosity of water was used in calculating Eq. 9 rather than the solution viscosity. As discussed earlier, the largest variation of solution concentration is from roughly 110 wppm at the centerline (at $x/d = 8$) to zero at the wall. Previously, McComb et al. (1977) found little difference between the effect of using the water viscosity or the solution viscosity (up to 100 wppm) to normalise spectra.

The local rate of turbulent energy dissipation was estimated from the spectral curves by fitting tangents, of slope equal to −5/3, by eye. Then corresponding values of $E(k)$ and $k$ were substituted in

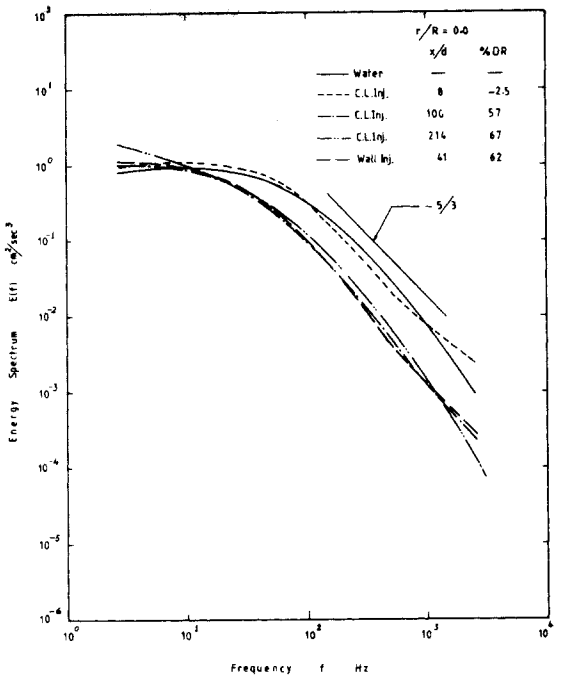


(a) Frequency spectra

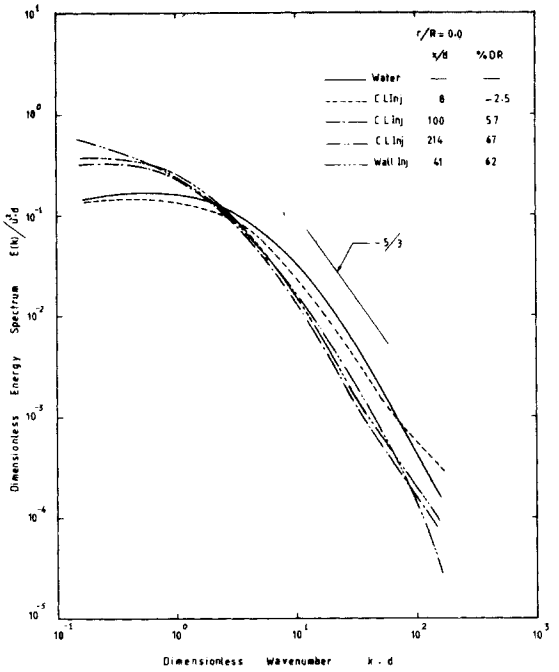


(b) Wavenumber spectra scaled by pipe flow parameters

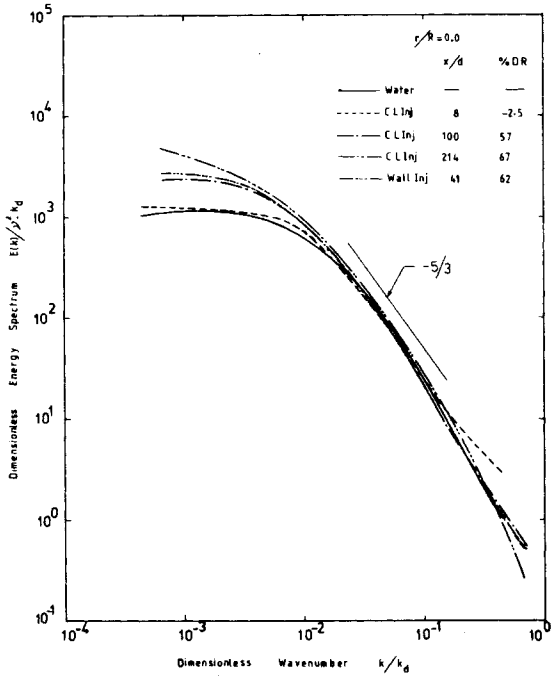


(c) Wavenumber spectra scaled by Kolmogoroff variables

**Figure 5. One-dimensional energy spectra at $r/R = 0$.**

the formula for the inertial subrange of the spectrum:

$$E(k) = F\epsilon^{2/3}k^{-5/3}, \tag{6}$$

where $F$ is a constant. Lawn (1971) found that $F = 0.53$ for pipe flows and this was the value used here.

Spectra measured at the centerline of the pipe are shown in Figure 5(a) in the frequency domain; and with both types of wavenumber scaling in Figures 5(b, c). All the spectra were tangent to a line of $-5/3$ slope for limited range of wavenumbers. Also, it was clear that the turbulent energy spectra in flows exhibiting drag reduction do show changes compared with those in water flows. When normalized using pipe-flow parameters as in Figure 5(b), these changes took the form of a shift of the spectral curve towards the low-frequency end. When scaled using Kolmogoroff variables as in Figure 5(c), the high wavenumber part of the spectrum (i.e., the inertial and dissipation ranges) in drag-reducing flows was identical to that in water, although there was still some enhancement of the energy-containing range. Evidently the suppression of small eddies was on the same scale as the reduction in wall shear stress. These changes in the energy spectrum were found to apply over the entire cross-section of the flow.

For a more quantitative comparison, Table 2 shows the rate of dissipation and the dissipation length and time scales for both water flow and flow with polymer injection. The results show a reduction in the centerline and wall region during drag reduction. An increase in the size and lifetime of dissipation eddies was observed in both the core region and the region near the wall.

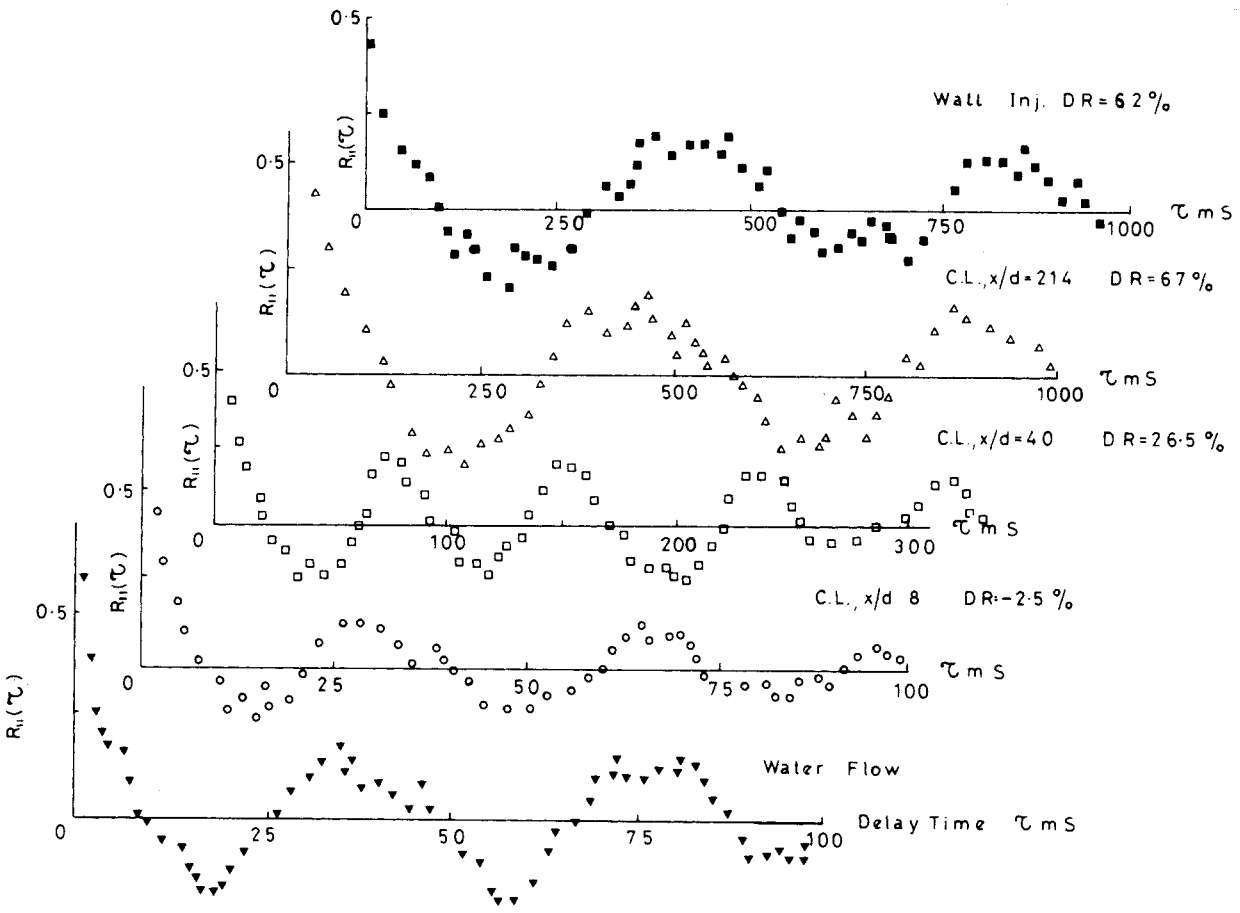


**Figure 6. $R_{11}(\tau)$ measured with short sample time to show the turbulent bursts.**

### Effect of Polymer Injection on Turbulent Bursts

The subject of turbulent bursts, and its importance in the context of drag reduction, is well known. The main parameter is the mean time between bursts $T_B$ (or the mean bursting period). We used the short-sampling time autocorrelation method to obtain $T_B$. This was first used by Kim et al. (1971) and developed by other workers (e.g., Strickland and Simpson, 1975; Mizushina and Usui, 1977). In this technique, individual values of the bursting period are calculated from the time between the zero order and first order peaks in $R_{11}(\tau)$. Then the mean bursting period $T_B$ may be calculated from a number of curves for $R_{11}(\tau)$. Figure 6 shows typical results for $R_{11}(\tau)$ taken at various levels of drag-reduction: note the change in scale of the time axis with increasing drag reduction.

Strickland and Simpson (1975) showed that the average of only 26 individual bursting times gave a satisfactory result, while Mizushina and Usui (1977) reported that $T_B$ obtained from 20 samples agreed well with the value obtained from 100 samples. In the present work, at least 20 individual values were used to calculate an average value for the bursting period at any radial position. As Figure 7 indicates, there was no systematic variation of the bursting period over the cross-section of the pipe. Thus, $T_B$ could be calculated as an average of more than 30 values of the bursting period, each calculated at different radial locations in the flow and each based on at least 20 realizations. The results of this process for both water flows with polymer injection may be seen in Table 3.

The results for water flow agree quite well with previous results for Newtonian flows. In particular, when scaled by outer flow parameters ($U$ and $R$ in our case), the bursting time should be independent of Reynolds number. Rao et al. (1971) found that $\overline{T}_B U/R = 5 \pm 2$, which agrees with the values given in Table 3.

The values of $T_B$ for flows with polymer injection show a very substantial increase over values for water flows, at quite moderate levels of drag reduction. It is interesting to note that this increase

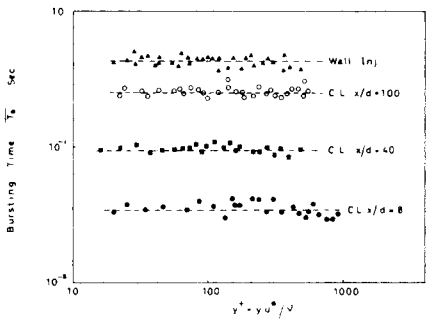


**Figure 7. Mean time between bursts as a function of radial position.**

is found even at the same wall shear stress: that is, even when scaled by wall region parameters. Increased bursting times in drag reducing flows have been reported previously (e.g., Achia and Thompson, 1977; Mizushina and Usui, 1977).

### NOTATION

| | |
|---|---|
| $A,B$ | = constants in universal logarithmic mean velocity profile, Eq. 1 |
| $C,D$ | = constants in logarithmic velocity distribution in polymerinteraction layer, Eq. 3 |
| $C_p,C_{av}$ | = polymer concentrations; master solution, bulk mean, wppm |
| $C_S$ | = salt (NaCl) concentration, wppm |
| $d$ | = pipe diameter |
| $E(k)$ | = one-dimensional turbulent energy spectrum |
| $f$ | = frequency, Hz |

$k$ = wavenumber
$k_d$ = Kolmogoroff dissipation wavenumber, $(= \epsilon^{1/4}/\nu^{3/4})$
$r$ = radial coordinate
$R$ = pipe radius
Re = Reynolds number
$R_{11}(\tau)$ = autocorrelation of streamwise fluctuating velocity
$T_B$ = mean time between bursts
$u^*$ = friction velocity
$u'$ = root-mean-square fluctuating velocity
$U, U^+$ = mean velocities, $(U^+ = U/u^*)$
$x$ = downstream distance ($x = 0$ at point of injection)
$y, y^+$ = distance from wall $(y^+ = yu^*/\nu)$

**Greek Letters**

$\epsilon$ = rate of energy dissipation
$\eta_d$ = dissipation length scale, $(= \nu^{3/4}/\epsilon^{1/4})$
$\nu$ = kinematic viscosity
$\tau$ = delay time in autocorrelation
$\tau_d$ = dissipation time scale $(= \nu^{1/2}/\epsilon^{1/2})$

## LITERATURE CITED


Achia, B. U., and D. W. Thompson, "Structure of the Turbulent Boundary in Drag-Reducing Pipe Flow," *J. Fluid Mech.*, **81**, 439 (1977).

Butson, J., and D. H. Glass, "Mass-Transfer Measurements in the Turbulent Pipe Flow of a Solution of Drag-Reducing Polymer," Paper A3 Proc. 1st Int. Conf. on Drag Reduction, Cambridge, U.K. (BHRA: 1974).

Chung, J. S., and W. P. Graebel, "Laser Anemometer Measurements of Turbulence in Non-Newtonian Pipe Flows," *Phys. Fluids*, **15**, 546 (1972).

George, W. K., and J. L. Lumley, "Laser-Doppler Velocimetry and Its Application to the Measurement of Turbulence," *J. Fluid Mech.*, **60**, 321 (1973).

Hanratty, T. J., L. G. Chorn and D. T. Hatziavramidis, "Turbulent Fluctuations in the Viscous Wall Region for Newtonian and Drag Reducing Fluids," *Phys. Fluids*, **20**, 5112 (1977).

Kim, H. T., S. J. Kline and W. C. Reynolds, "The Production of Turbulence Near Smooth Wall in a Turbulent Boundary Layer," *J. Fluid Mech.*, **50**, 133 (1971).

Lawn, C. J., "The Determination of the Rate of Dissipation in Turbulent Pipe Flow," *J. Fluid Mech.*, **48**, 477 (1971).

Logan, S. E., "Laser Velocimeter Measurement of Reynolds Stress and Turbulence in Dilute Polymer Solutions," *AIAA J.*, **10**, 962 (1972).

McComb, W. D., J. Allan and C. A. Greated, "Effect of Polymer Additives on the Small-Scale Structure of Grid-Generated Turbulence," *Phys. Fluids*, **20**, 873 (1977).

McComb, W. D., and L. H. Rabie, "Local Drag Reduction due to the Injection of Polymer Solutions into Turbulent Flow in a Pipe: Part I. Dependence on Local Polymer Concentration," *AIChE J.* (July, 1982).

Mizushina, T., and H. Usui, "Reduction of Eddy Diffusion for Momentum and Heat in Viscoelastic Fluid in a Circular Tube," *Phys. Fluids*, **20**, S100 (1977).

Rabie, L. H., "Drag Reduction in Turbulent Shear Flow Due to Injected Polymer Solutions," PhD. Thesis, Edinburgh University (1978).

Rao, N. K., R. Narasimha, and M. E. Badri Narayanan, "The 'Bursting' Phenomenon in a Turbulent Boundary Layer," *J. Fluid Mech.*, **48**, 339 (1971).

Reischman, M. M., and W. G. Tiederman, "Laser-Doppler Anemometer Measurements in Drag-Reducing Channel Flows," *J. Fluid Mech.*, **70**, 369 (1975).

Rudd, M. J., "Laser Dopplermeter and Polymer Drag Reduction," *Chem. Eng. Prog. Symp. Ser.*, No. 111, **67**, 21 (1971).

Strickland, J. H., and R. L. Simpson, " 'Bursting' Frequencies Obtained from Wall Shear Stress Fluctuations in a Turbulent Boundary Layer," *Phys. Fluids*, **18**, 306 (1975).

Virk, P. W., H. S. Mickley, and K. A. Smith, "The Ultimate Asymptote and Mean Flow Structure in Toms Phenomenon," *ASME J. Appl. Mech.*, **37**, 488 (1970).



*Manuscript received April 6, 1981; revision received September 22, and accepted October 13, 1981.*


# Further Work on Multicomponent Liquid Phase Adsorption in Fixed Beds


**SHU-CHIEH WANG and CHI TIEN**

**Department of Chemical Engineering and Materials Science**
**Syracuse University, Syracuse, NY 13210**



**The problem of multicomponent liquid phase adsorption in fixed beds was studied further. In contrast to the earlier work (Hsieh et al., 1977), the method developed in this work is more efficient and also has a greater scope of applicability as it incorporates the use of the IAS (Ideal Adsorbed Solution Theory) method for the estimation of multicomponent adsorption equilibrium data. It was shown that the use of the more complex IAS method for the prediction of the isotherm data does not present insurmountable obstacles as once feared (DiGiano, 1978) but provides much better prediction of carbon adsorption. An extension of the method to batch adsorption was shown to be straightforward and presented no special difficulty.**


## SCOPE

This study further develops the numerical technique necessary for the solution of multicomponent liquid phase adsorption in fixed beds. Although a general method for the solution of this problem is already available (Hsieh et al., 1977) this earlier developed method was found to experience convergence difficulty if the number of adsorbable species involved is large and/or if the rate controlling step of the adsorption process is a combination of the liquid and particle phase mass transfer resistances. Furthermore, it was limited to systems whose equilibrium relationships are of the Langmuir type.

The method developed in this work is free of the convergence difficulty. Furthermore, it is developed to incorporate the use of the IAS method for the prediction of the isotherm data, which


Correspondence concerning this paper should be addressed to C. Tien. S.-C. Wang is with Washington Research Center, Columbia, MD.